Viser Technology Pte. Ltd.
Research and Application of Materials Science
DOI: 10.33142/rams.v5i2.12705

Research Article Open Access

The Influence of Dry or Wet Activating Process to the Electrochemical Features of Biowaste Carbon

Zhonghe SONG[1], Yanmei ZHAO[2], Shangwen MA[3], Tiezhen REN [1, 3*]

1. School of Chemical Engineering, Xinjiang University, Urumqi, Xinjiang, 830046,China
2. School of Chemical Engineering, Hebei University of Technology, Tianjin, 300130, China
3. Bayingol Vocational and Technical School, Korla, Xinjiang, 841000, China

[*]***Corresponding Author:*** *Tiezhen REN, E-mail: rtz@xju.edu.cn*

Abstract

The utilization of biowaste to the activated carbon (AC) as electrode material is conducive to alleviating the energy crisis and promoting the high value-added. The popular KOH activation has been applied for years, but rare report clarified the difference of dry and wet activation, with which the batch producing technique could be different. Here nitrogen doped hierarchical AC was derived from wood chip by a wet or dry KOH activation. The surface area, framework structure and surface feature were characterized to reveal the effect of wet and dry activation. 1.44 at% of nitrogen doped AC was made by dry KOH activation, which was higher than the AC derived from wet KOH activation with 1.36 at% of nitrogen. Their electrochemical properties were investigated in 6 mol L^{-1} of KOH, the capacitance of wAC was 401 F g^{-1} at 0.5 A g^{-1}, but dAC possessed a capacitance of 215 F g^{-1}. These indicated that AC obtained by using wet KOH activation displayed a potential application in energy field.

Keywords: *Activated carbon; KOH activation process; supercapacitor*

1 Introduction

Biowaste-derived activated carbon (AC) has been widely used in adsorbents[1,2], electrocatalysts[3,4] and other fields with possessed features, such as high specific surface area, flexible pore size distribution and adjustable surface features with heteroatoms[5]. Specially, their functional groups and morphological characteristics are closely related to the electrochemical performance by enhancing the diffusion of electrolyte ions [6]. As a double-layer capacitance, the cycle life of AC electrode is often higher than the metal oxides, which was ascribed to the pseudocapacitor [7]. It is confirmed that the micropores determine the space for charge storage and the reasonable pore structures decide the kinetics of current charging and discharging [8]. While, to meet the demand for industrial mass production the technology challenges the activation process of KOH.

Some reports adopted dry-mixing or wet-mixing KOH activation to obtain the AC [9-10]. Under the premise of ensuring catalysts active, a higher requirement is putting forward to reducing the amount of KOH. By 9 mass ratio of wet KOH activation, AC derived from willow wood displayed a surface area of 2800 m^2 g^{-1} and a capacitance of 394 F g^{-1} at 1 A g^{-1}[9]. The Celery-derived AC with polyaniline as a nitrogen source was prepared by four-times of KOH solution[11], which capacitance could reach to 402 F g^{-1} in H_2SO_4 (1 mol L^{-1}) at 1 A g^{-1}. However, the differences of microporous structure and functional group contents in carbon might affect the electrochemical feature and the biomass sources are unique with a specific activation process for their own [12]. It is still in question for limiting the consumption of KOH and finding a matched activation technique.

Here, KOH activation by dry or wet mixing have been chosen to construct nitrogen doped AC from wood chip. The physical feature was characterized and the pore structure was discussed to illustrate the effect of activation process. The related capacitance was evaluated with cyclic voltammetry (CV) test and charging-discharging performance in a two-electrode system. The results could highlight the activating technique for batch production of AC in the future.

2 Experimental Details

All the chemicals purchased from Sigma Aldrich Co. Ltd was directly used without any pretreatment. Wood

Received on October 6, 2023; Accepted on November 14, 2023

chip was collected from Korla, Xinjiang and cleaned with water to remove the surface dust.

2.1 Preparation process

First, 5 g of wood chip was carbonized in nitrogen flow (60 mL min^{-1}) in a tube furnace at 500 ℃ for 2 h, for which 10 ℃ min^{-1} of rate was kept from room temperature to final. Then the collected sample was mixed with two mass ratios of KOH. For wet KOH activation, 20 ml of distilled water was added and stirred overnight for 12 h, following the activation was set at 800 ℃ for 2 h with same setting program. For dry KOH activation, the KOH is fully grinded with the carbonized AC for half an hour. After activation, all the samples were neutralized with 1 mol L^{-1} of HCl and distilled water. Finally, drying them in the oven at 80 ℃ and the collected sample was named wAC and dAC, respectively.

2.2 Characterizations

To understand the porous feature of the sample, nitrogen adsorption-desorption isotherms analyzer (Quantachrome Autosorb-1 MP) were taken at liquid-N_2 temperature (-196 ℃). The surface area was calculated by Brunauer-Emmett-Teller (BET) method and pore size distribution was deduced by Non-Local Density Functional Theory (NLDFT) [13]. The morphology of the samples was observed from scanning electron microscope (SEM, JSM-6490LV); Transmission electron microscope (TEM, JEM 1010) was used to record the microstructure. Raman scattering spectra were recorded by Renishaw InVia with 532 nm excitation light source. To reveal the detail surface structure, the X-ray photoelectron spectroscopy (XPS, Thermo ESCALAB 250) was taken with irradiation source monochromatic Al Kα radiation (150 W, 15 kV, and 1486.6 eV) in an evacuated chamber ($5.2*10^{-9}$ mbar). High resolution spectra were performed to explore the local environment of each element at a fixed angle of 90 º. C1s (284.6 eV) was used to calibrate the energy scale.

2.3 Electrochemical tests

Nickel foam was selected as working electrode collector with $1cm^2$ active area. Ethanol was used as the dispersible solvent. 10 mg of sample was first mixed with acetylene black and polytetrafluoroethylene (60 wt%), by keeping a mass ratio of 75:25:5. Then the mixture was pressed under 20 MPa for 20 s to form the electrode. Before test, the work electrode was fully infiltrated in KOH electrolyte (6 mol L^{-1}) for 10 h. The galvanostatic discharge-charge cycling tests were measured on LAND testing system.

Cyclic voltammetry (CV, -1 to 0 V) and electrochemical impedance spectroscopy (EIS, 10 mHz to 100 kHz) were tested by an electrochemical workstation (IM6&ZENNIUM). Three electrode system was designed with a reference electrode Hg/HgO and the counter electrode was a platinum electrode in KOH electrolyte (6 mol L^{-1}). EIS was recorded at open circuit voltage under disturbance voltage of 5 mV.

The specific capacitance of the two-electrode system was obtained with the equation (1). The energy density (E) and power density (P) were derived from the equation (2) and (3).

Equation:

$$\boldsymbol{C = \frac{2I\Delta t}{m\Delta V}} \quad (1)$$

$$\boldsymbol{E = \frac{1}{2*3.6} C\Delta V^2} \quad (2)$$

$$\boldsymbol{P = \frac{3600E}{\Delta t}} \quad (3)$$

Where C (F g^{-1}) relates to the specific capacitance, I (A) is the electric current, Δt (s) is the discharge time, m (g) is the mass of active carbon, ΔV (V) is potential difference, E (Wh kg^{-1} is energy density, P (W kg^{-1}) is power density.

3 Results and Discussions

N_2 adsorption-desorption isotherm was shown in Figure 1a. The calculated S_{BET} of wAC is 1793 $m^2 g^{-1}$ with the total volume (V_{total}) of 1.045 $cm^3 g^{-1}$. While, S_{BET} of dAC is 1429 $m^2 g^{-1}$ with the V_{total} of 0.703 $cm^3 g^{-1}$. According to the NLDFT method[13], the pore size distribution of wAC mainly locates at around 0.59 and 1.67 nm. For dAC, the pore size is around 0.59 nm and 1.48 nm, as represented in Figure 1b. The results indicate that wet KOH activation could be helpful to obtain the carbon with a higher SSA and larger pore volume than dry KOH activation. We believe that, due to the KOH solution is fully impregnated into the pores of the carbonized material, wAC with a richer microporous structure. Raman spectra revealed the structure of AC with the ratio of G band (1600 cm^{-1} fitting to graphite structure, sp^2) and D band (1350 cm^{-1} fitting to amorphous structure, sp^3)[14]. As represented in Figure 1c, more defects exist in wAC corresponding to the I_D/I_G values of 1.07 (dAC with 1.05), which confirm that the wet KOH causes more amorphous carbon structure than that through dry activation. The pores in carbon framework could be immersed thoroughly with KOH solution. The SEM images of dAC displayed an irregular structure like megalithic array (Figure 1d). But wAC showed a cauliflower-like morphology (Figure 1e), suggesting that the activation in solution is vigorous comparing to grinding way. TEM images display the irregular micropores as shown in Figure 1f and 1g. The related inset images clearly show that the abundant pore structure in wAC.

The function groups of the samples were investigated by XPS (Figure 2a). The elements of C1s,

N1s and O1s existed in wAC and dAC. There are more C1s (89.49 at%) contained in dAC, which is slightly higher than wAC (88.79 at%). dAC has 9.06 at% O1s less than wAC (9.85 at%). High content of nitrogen is formed during dry KOH activation (1.44 at%), comparing to wAC (1.35 at%). The C 1s spectra of the samples at around 284.6, 285.5, 286.8 and 289.1 eV are assigned into four bonding configurations, C=C, C-O/C-N, C=O/C=N and O-C=O, as represented in Figure 2b. The O1s core energy level spectra is at around 531.5, 532.5, 533.7, and 534.7 eV, fitting to the group of O=C, O-C, O-N, and water or chemisorbed O_2/CO_2 [15] in Figure 2c.

N1s spectra in Figure 2d, is at around 398.8, 399.8, 401.6 and 403.1 eV, which represent four groups of pyridine-N, pyrrole-N, graphitic-N and pyridine N^+-O^-. The wet activation process may introduce more pyrrolic-N (0.65 at%). While dry activation represents more pyridine-N (0.69 at%) and no pyridine N^+-O^- groups. This suggests that the activation process not only affect the surface feature and porous structure, the nitrogen species might be tuned during the activation. Since the alkali solution is more thoroughly interacted with carbon atoms and more functional groups could be formed, the design on heteroatoms type might be successful. All peaks information had been summarized in Table1.

The elecochemical nature of dAC and cAC was discussed through the CV curves. The large square area is obvious for wAC, indicating that rich micropores in wAC contribute to a good performance in electric double layer capacitance (Figure 3a, 3b).

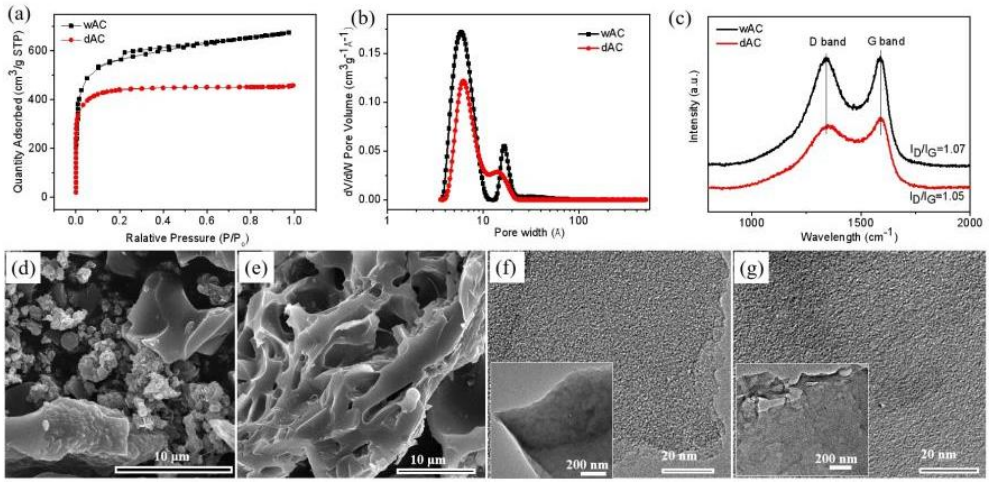

Figure 1 N_2 adsorption-desorption isotherms (a) and pore size distribution (b), Raman spectra (c), SEM images (d) and (e), TEM images (f) and (g) of dAC and wAC

Table 1 The summary of quantitative elements and the fitting peak information of the wAC and dAC by XPS

Bond assignment	Binding energy (eV)	wAC (at.%)	dAC (at.%)
C1s		88.79	89.49
C=C sp^2	284.6	57.12	58.18
C-O (phenolic, alcoholic, ether), C–N (carbon–nitrogen structures)	285.5	8.39	8.10
O-C=O (carboxyl or ester)	286.8	10.09	9.36
π→π*, π-electrons in aromatic rings	289.1	13.19	13.85
O 1s		9.85	9.06
O=C (in carboxyl/carbonyl)	531.5	4.05	3.92
O-C (in phenol/epoxy)	532.5	3.14	2.55
N-O	533.7	1.83	1.60
Water or chemisorbed O_2, CO_2	534.7	0.83	0.99
N 1s		1.36	1.44
pyridine-N	398.8	0.30	0.69
pyrrole-N	399.8	0.65	0.48
graphitic-N	401.6	0.27	0.27
pyridine N^+-O^-	403.1	0.14	---

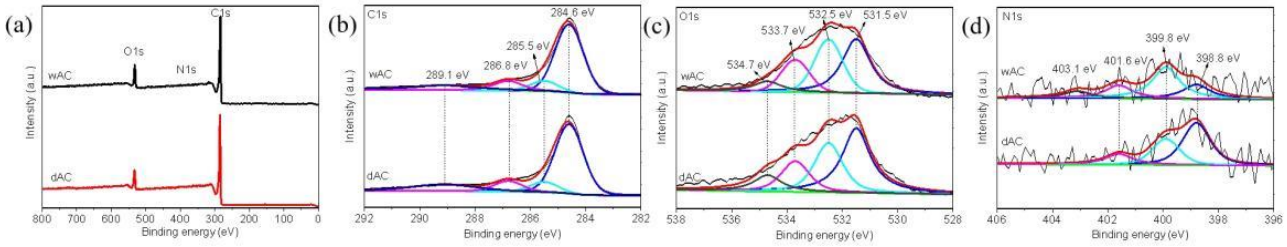

Figure 2 The XPS survey spectra (a) and high-resolution core energy level spectra of C1 (b), O1s (c), and N1s (d) of dAC and wAC

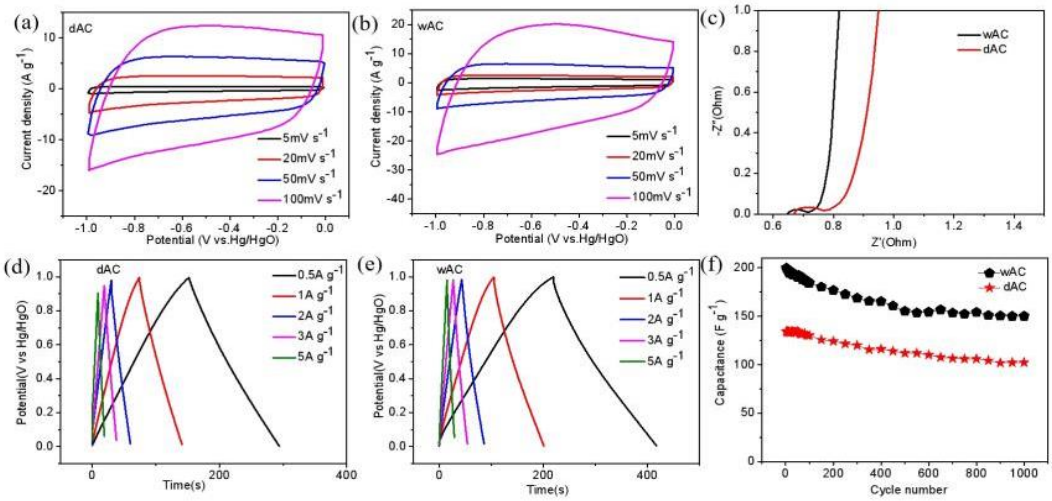

Figure 3 Cyclic voltammetry (CV) curves of dAC (a) and wAC (b), the Nyquist plots in a three-electrode system of dAC and wAC (c), the GCD curves of dAC (d) and wAC (e) in a two-electrode cell, the cycle life test at1A g^{-1} of dAC and wAC (f)

The EIS was recorded at the open circuit voltage in Nyquist plot (Figure 3c). The curves of the samples display a semi-arc and a straight line, which might be ascribed to the dynamic processes of charge transfer and mass transfer[16]. The wAC possesses a small semicircle diameter than dAC, indicating a low electrical resistance and good electrical conductivity. This must be contributed by microporous structure and nitrogen doped. Then the two-electrode system of the GCD tests were recorded in 6 mol L^{-1} of KOH. the curves in Figure 3d and 3e keep the typical triangular shape at different current density. It is obvious that the wAC shows a long charging-discharging time. The calculated capacitance of wAC and dAC from equation (1) is 200 and 134 F g^{-1} at 1 A g^{-1}. The capacitance of the samples is comparable with some literatures [17-21], which are summarized in Table 2. We may see that bio-precursors possess different surface area and capacitance even with same activating dosage. Thus, preparing AC with electrochemical feature needs to load a specific procedure for their own.

The related energy density and power density were obtained from equation (2) and (3). The wAC has a high energy density of 55 Wh kg^{-1} and power density of 1980 W kg^{-1}. This result is better than mesopores AC with Black locust seed dregs as the carbon source, its energy density is 26.2 Wh kg^{-1} and power density is 790 W kg^{-1}[22]. Cyclic stability was measured by GCD at 1 A g^{-1}. From Figure 3f, wAC electrode has the capacitance retention 75.5% after 1000 cycles GCD test, and the nearly capacitance retention 76.1% in dAC. Obviously, dry mixing is inadequate in contacting the inner surface of carbon [23]. The wet mixing activation consumes an immersion residence time, that may guarantee the carbon precursor sufficiently absorb KOH to create a functional carbon material.

Table 2 Summary of capacitance performances of carbon materials reported in various literature studies in 6 mol L^{-1} of KOH at three electrode system

Materials	KOH ratio*	Activating method	S_{BET} (m^2 g^{-1})	C (F g^{-1}) #	Refs.
Soy root	4	wet	2690	328	[17]
Natural casings	4	wet	2512	290	[18]
White sugar	3	wet	713	242	[19]
pectin	2	wet	2928	338	[20]
Tea leaves	2	dry	912	167	[21]
Wood chips	2	dry	1429	191	This work
	2	wet	1793	289	

The capacitance was recorded at 1A g^{-1}.

4 Conclusion

In this paper, nitrogen-doped AC was obtained from wood chips by wet and dry activation processes with KOH. A low surface area could be obtained during dry activation with 1429 $m^2 g^{-1}$, but with high content of nitrogen (1.44 at%). On the contrary, wAC possessed a surface area of 1793 $m^2 g^{-1}$ and the nitrogen retention is1.36 at%. For nitrogen species, pyridine-N in dAC is 0.69 at%, higher than that of wAC (0.3 at%). While, pyrrole-N in dAC is 0.48 at%, lower than that of wAC (0.65 at%). As a consequence, 200 F g^{-1} could be reached for wAC, which is higher than dAC (134 F g^{-1}). Meanwhile, wAC has an energy density of 26.6 Wh kg^{-1} at a power density of 484 W kg^{-1}, which is higher than commercial activated carbon. The wet activation promotes large surface area and rich micropores. Although more nitrogen element may loss during the activation process, more oxygen-containing groups are embedded in carbon framework, which may provide predictable benefits for designing the expected carbon framework. We confirm that the wet activation method has obvious advantages over the dry activation method as an efficient bulk processing technique.

Acknowledgement: This work was supported by the Natural Science Foundation of Xinjiang Uygur Autonomous Region (2021D01A03), Project of Tian chi talent leader in Xinjiang Uygur Autonomous Region (2022).

References

[1]Lan Luo. Construction of ultra-microporous activated carbons derived from waste distiller's grains for efficient CO2 adsorption[J]. SEP PURIF TECHNOL, 2022(302):122134.

[2]Chian Ying Teo. Carbon-Based Materials as Effective Adsorbents for the Removal of Pharmaceutical Compounds from Aqueous Solution[J]. Adsorp Sci Technol, 2022(400):3079663.

[3]Xueping Sun. Novel transition-metal phosphides@N, P-codoped carbon electrocatalysts synthesized via a universal strategy for overall water splitting[J]. J. Alloys Compd, 2023(932):167253.

[4]Sanket D, Bhoyate,. Science and engineering for non-noble-metal-based electrocatalysts to boost their ORR performance: A critical review[J]. Coordin Chem Rev, 2023(474):214854.

[5]Yiliang Wang. Biomass-Derived Carbon Materials: Controllable Preparation and Versatile Applications[J]. SMALL, 2021(17): 2008079.

[6]Jiangqi Zhou. Biomass-Derived Carbon Materials for High-Performance Supercapacitors: Current Status and Perspective[J]. Electrochem. Energ Rev, 2021(4):219–248.

[7]Chunyu Zhang. Selective H2O2 Electrosynthesis over Defective Carbon from Electrochemical Etching of Molybdenum Carbide[J]. ACS Appl Mater Interfaces, 2023(15):838–847.

[8]Yunxian Zhang. Regulable pyrrolic-N-doped carbon materials as an efficient electrocatalyst for selective O2 reduction to H2O2[J]. New J Chem, 2022(46):14510-14516.

[9]Zhanyong Li. Preparation of activated carbons from poplar wood by chemical activation with KOH[J]. J Porous Mater, 2017(24):193–202.

[10]Jingjiang Liu. Promising nitrogen-rich porous carbons derived from one-step calcium chloride activation of biomass-based waste for high performance supercapacitors[J]. ACS Sustain. Chem. Eng, 2026(4):177-187.

[11]Wei Du. Nitrogen-doped hierarchical porous carbon using biomass-derived activated carbon/carbonized polyaniline composites for supercapacitor electrodes[J]. Journal of Electroanalytical Chemistry, 2018(827):213-220.

[12]Yan Zhang. Insights into the KOH activation parameters in the preparation of corncob-based microporous carbon for high-performance supercapacitors[J]. Diam Relat Mater, 2022(129):109331.

[13]John Landers. Density functional theory methods for characterization of porous materials[J]. Colloid Surface A, 2013(437):3-32.

[14]Xuelin Zhang. Heteroatom-doped porous carbons derived from moxa floss of different storage years for supercapacitors[J]. RSC Advances, 2018(8):16433-16443.

[15]hanshan Xu. Nitrogen-containing activated carbon of improved electrochemical performance derived from cotton stalks using indirect chemical activation[J]. Colloid Interface Sci, 2019(540): 285-294.

[16]Bin Wang. A simple and universal method for preparing N, S co-doped biomass derived carbon with superior performance in supercapacitors[J]. Electrochimica Acta, 2019(309):34-43.

[17]Nannan Guo. Interconnected and hierarchical porous carbon derived from soybean root for ultrahigh rate supercapacitors[J]. J Alloy Compd, 2020(834):155115.

[18]Zongying Xu. N-enriched multilayered porous carbon derived from natural casings for high-performance supercapacitors[J]. Applied Surface Science, 2018(444): 661-671.

[19]Kabir.O. Oyedotun. Examination of high porosity activated carbon obtained from dehydration of white sugar for electrochemical capacitor applications[J]. ACS Sustainable Chemistry & Engineering, 2019(7):537–546.

[20]Yuhao Zhou. In-situ template cooperated with urea to construct pectin-derived hierarchical porous carbon with optimized pore structure for supercapacitor[J]. Electrochim. Acta, 2020(355):13681.

[21] Xinyu Song. Tea waste derived microporous active carbon with enhanced double-layer supercapacitor behaviors[J]. Applied Surface Science, 2019(487):189-197.

[22]Lijie Hou. Hierarchically porous and heteroatom self-doped graphitic biomass carbon for supercapacitors[J]. Colloid Surface A, 2019(540):88-96.

[23]Pengfei Zhang. Ultrahigh surface area carbon from carbonated beverages: combining self-templating process and in situ activation[J]. Carbon, 2015(93):39-47.